



Full length article

## Identification of recycling pathways for secondary aluminum dross with integrated hybrid life cycle assessment

Luying Xiao<sup>a</sup>, Yao Wang<sup>a,b,\*</sup>, Rufeng Zheng<sup>a</sup>, Jingru Liu<sup>c</sup>, Jun Zhao<sup>a</sup>, Tek Maraseni<sup>d</sup>, Guangren Qian<sup>a,\*</sup>

<sup>a</sup> SHU Center of Green Urban Mining & Industry Ecology, School of Environmental and Chemical Engineering, Shanghai University, 381 Nanchen Road, 200444, Shanghai China

<sup>b</sup> Shanghai Institute of Geological Survey, 930 Lingshi Rd, 200072, Shanghai China

<sup>c</sup> State Key Laboratory of Urban and Regional Ecology, Research Centre for Eco-Environmental Sciences, Chinese Academy of Sciences, 100085, Beijing, China

<sup>d</sup> Centre for Sustainable Agricultural Systems, University of Southern Queensland, 487/521-535 West Street, Darling Heights QLD 4350, Australia



## ARTICLE INFO

## Keywords:

Secondary aluminum dross  
Integrated hybrid life cycle assessment  
Sustainability  
Environmental impact

## ABSTRACT

The development of secondary aluminum dross (SAD) has become a hot topic to deal with aluminum resource scarcity and landfill risk as hazardous waste. This study first compares the environmental impact, resource consumption, and economic performance of four emerging SAD reutilization methods with an integrated hybrid life cycle assessment (IHLCA). The results show that IHLCA captures larger environmental and economic impacts than process LCA (PLCA), especially for midpoint indicators, such as human toxicity potential, acidification potential, freshwater aquatic ecotoxicity. Furthermore, multi-component recovery from SAD is not always the best choice. The multi-component recovery scenario of SAD-to-alumina with alkali has the smallest environmental impact and resource consumption, while SAD-to-PAC with acid is the worst due to the massive use of HCl. Particularly, SAD-to-calcium aluminate with single-component recovery stands out due to its best economic performance. The given results provide new perspective on making a sustainable decision for SAD recovery industrialization.

## 1. Introduction

Aluminum, as a major metal, enables transportation, housing, communication, and almost infinite array of products and services, the demand for which doubles or triples relative to 2010 levels by mid-century (Elshkaki et al., 2018). However, the increasing global demand for high-quality bauxite is unlikely to be sustainably met by the known reserves (Meyer, 2004) resulting in the rapid development of the global secondary aluminum production sector, which has grown steadily more than three times in the period of 1980–2007 (Maung et al., 2017). China, the world's largest primary aluminum producer and consumer country, accounting for 59.6% of the world's total primary aluminum production (Li et al., 2020), begins to enter the era of scrap aluminum recycling. During 2007–2019, the output of secondary aluminum rose tenfold in China (Ding et al., 2021). Aluminum dross, a waste rich in metallic content generated during industry processes, is also an important raw material in secondary aluminum production sector for recycling aluminum and other valuable products (Meshram and Singh, 2018;

Padamata et al., 2021). However, the metal recycling flows from currently available secondary aluminum recovery technologies meet only a modest fraction of metal demand.

The secondary aluminum dross (SAD) left after the aluminum recovery from primary aluminum dross has attracted attention from the secondary aluminum production industry in China with its generation of around 6 million tons in 2021 (Zhang, 2021). According to the National Catalogue of Hazardous Wastes (2021 Edition), SAD has been classified as a hazardous waste due to its hazardous properties of releasing ammonia by reacting with water (Li et al., 2012; Meyer, 2004; Zhao et al., 2022) and its high leaching toxicity caused by fluorides and chlorides (Hazar et al., 2005; Mahinroosta and Allahverdi, 2018). Nonetheless, SAD is a potential available resource with composition of  $\alpha\text{-Al}_2\text{O}_3$  (30–50%), AlN (2–10%), Al (2–10%) (Dash et al., 2008). The aluminum in SAD can be recycled as alumina by pyrometallurgical (Tenorio and Espinosa, 2002) and hydrometallurgical processes (Meshram and Singh, 2018; Ünlü and Drouet, 2002), and SAD-to-alumina with alkali is reported as promising hydrometallurgical

\* Corresponding authors.

E-mail addresses: [wangyaobmp@shu.edu.cn](mailto:wangyaobmp@shu.edu.cn) (Y. Wang), [grqian@shu.edu.cn](mailto:grqian@shu.edu.cn) (G. Qian).

<https://doi.org/10.1016/j.resconrec.2023.106987>

Received 10 December 2022; Received in revised form 22 February 2023; Accepted 30 March 2023

Available online 4 April 2023

0921-3449/© 2023 Elsevier B.V. All rights reserved.

processes (Zhu and Jin, 2021). Furthermore, considering the abundant  $\alpha\text{-Al}_2\text{O}_3$  in SAD with good chemical stability, SAD has been used to generate building materials such as non-fired bricks and concrete bricks (Kuo Cheng et al., 2013; Ni et al., 2021). With the development and wide application of flocculants, using SAD through hydrochloric acid leaching and calcium aluminate addition to produce flocculants such as poly aluminum chloride (PAC) has also been studied by many researchers (Li et al., 2010; Yang et al., 2010; Zarchi et al., 2013). Besides, calcium aluminate preparation approach were investigated by calcining a mixture of SAD and lime (Hu et al., 2021), while the technology for the distillation of aluminum isopropoxide from the solid-liquid reaction between aluminum metal and isopropyl alcohol was also developed (Yoo et al., 2006).

It is well known that the recycling of SAD could not only fulfill the gap in aluminum metal demand but also reduce the environmental threat caused by landfills (Padamata et al., 2021). Furthermore, the environmental and economic superiority of producing alumina from SAD over the traditional bauxite process has been reported, with 32.16% lower environmental impacts and 50.45% lower economic costs (Zhu et al., 2020). However, life cycle assessment (LCA) has been used to assess the environmental and economic performance of SAD reutilization technologies, but not to a great extent. Hong et al. (2010) and Hiraki et al. (2005) quantified the energy consumption and carbon dioxide emissions of SAD deactivation and alumina extraction which only focus on the high temperature processing methods and limited impact categories. Zhu and Jin (2021) found that the ball milling scenario had the smallest environmental impacts, and the alkali scenario had the highest economic profit, both of which focus on alumina recovery with other reutilization methods ignored, such as Al-containing chemical products or bricks. Notably, these studies are limited to traditional process-based LCA, which excludes many upstream processes due to difficulties in collecting inventory data on all inputs (e.g., technical and financial services) at the process level (Li et al., 2020). As a result, traditional process-based LCA suffers from system truncations, and the environmental impacts are underestimated. In contrast, the integrated hybrid life cycle assessment (IHLCA) has been proven to avoid system truncation by constructing upstream and downstream matrices to expand the system boundary to the whole economy (Palma-Rojas et al., 2015; Suh and Huppel, 2005; Wiedmann et al., 2011). Zheng et al. (2022) found that the neglected impact in global warming, primary energy demand and human toxicity from the economic input-output (EIO) system of municipal solid waste incineration fly ash reutilization scenarios account for 15–53%, 26–65%, and 93–96% of total impacts, respectively. Additionally, a significant role of the EIO systems, which contribute about 60% of the life cycle energy consumption throughout the shale gas supply chain, was also observed (Gao and You, 2017). Therefore, it is of great concern to determine the environmental and economic superiority of SAD reutilization scenarios covering different types of recycled products with the IHLCA model.

Consequently, the main goal of this study was to compare the environmental impact, resource consumption and economic performance of various SAD reutilization methods using IHLCA model. Four emerging SAD reutilization scenarios that are widely used in China were evaluated in this study: SAD-to-calcium aluminate, SAD-to-concrete brick, SAD-to-PAC with acid, and SAD-to-alumina with alkali. Then global sensitivity analysis and uncertainty analysis based on Monte Carlo simulation was conducted to identify the reliability of the results and key parameters for SAD reutilization technology improvements.

## 2. Materials and methods

### 2.1. Goal and scope

In this work, we conduct IHLCA studies of four SAD reutilization scenarios, namely SAD-to-calcium aluminate, SAD-to-concrete brick, SAD-to-PAC with acid and SAD-to-alumina with alkali. Due to various

products generated by each SAD reutilization technology, the function unit is set as the reutilization of 1 t SAD. All materials, energy consumption, emissions, waste disposal, and economic costs were based on this functional unit.

Fig. 1 depicts the structure of IHLCA model for SAD reutilization, including process systems, EIO systems, downstream cutoff flows, and upstream cutoff flows. For process systems (Figure A1.1.), the system boundary is set based on "grave-to-cradle" thinking, which starts with the generated SAD being transported to a reutilization plant, and ends in final products leave factory. Since the metal aluminum recovery from SAD until 1 wt% left is similar in four SAD reutilization scenarios (Zhu and Jin, 2021), this process was not included in this study. For EIO-LCA part, this study adopts the *China Input-Output Table 2012*. To avoid errors due to allocation, the products, including calcium aluminate powder, concrete bricks, PAC, alumina, etc., are deducted from the original system as an offset considered equivalent to traditional products (Viau et al., 2020).

The four SAD scenarios can be classified according to the chemical components recycled.

- S1 (SAD-to-calcium aluminate) is a single-component recovery scenario in which the active aluminum components in SAD react with calcite through calcination in rotary kilns to produce calcium aluminate.
- S2 (SAD-to-concrete brick) is a two-component recovery scenario that separates aluminum and nitrogen elements by catalytic hydrolysis and produces concrete brick and ammonium sulfate, respectively.
- S3 (SAD-to-PAC with acid) is a multi-component recovery scenario that includes the recycling of aluminum, nitrogen, and fluorine. In this scenario, acid is used to dissolve alumina in SAD for PAC production, while generating  $\text{CaF}_2$  and ammonia water as by-products.
- S4 (SAD-to-alumina with alkali) is another multi-component recovery scenario with aluminum, nitrogen, and fluorine elements reutilized. In this scenario, alkali is used to extract alumina from SAD, and meanwhile, it generates  $\text{CaF}_2$ , ammonium sulfate,  $\text{NaCl}$ , and  $\text{KCl}$  as by-products.

### 2.2. Life cycle inventory analysis

To conduct the IHLCA of SAD reutilization, both bottom-up process data and Chinese Environmentally Extended Input-Output (CEEIO) data are required. Firstly, the zero burden of SAD assumption is used for life cycle inventory data collection (Huber and Fellner, 2018), and we selected the year 2012 as the baseline in this study. Then, to obtain the input-output data of four SAD reutilization technologies, we conducted a field tracking survey of four long-term operating enterprises, which are located in Henan Gongyi (SAD-to-calcium aluminate, SAD-to-alumina with alkali), Zhejiang Dongyang (SAD-to-concrete brick), and Zhejiang Changxing (SAD-to-PAC with acid). Notably, the collected industrial data are basically consistent with the existing literatures (Zhu and Jin, 2021; Zhu et al., 2020). Thirdly, to track the destination of recyclable elements and pollutants, a transfer coefficient model was established according to the original mass balance in the collected inventory data. Furthermore, the methods outlined in Appendix 2 were used to supplement the ignored pollutants emissions by enterprise monitoring, such as  $\text{CO}_2$ , natural gas combustion emissions, and steam loss. The input-output inventory of four SAD reutilization scenarios was finally established (Appendix 1, Table A1.1). Notably, the CEEIO database 2012 developed by Liang et al. (2017) was used to construct IHLCA model, which consist of 139 industry sectors and 139 commodity sectors following the form of the *China Input-Output Table 2012*.

### 2.3. Integrated hybrid LCA model

In the IHLCA model, detailed process analysis is conducted to esti-

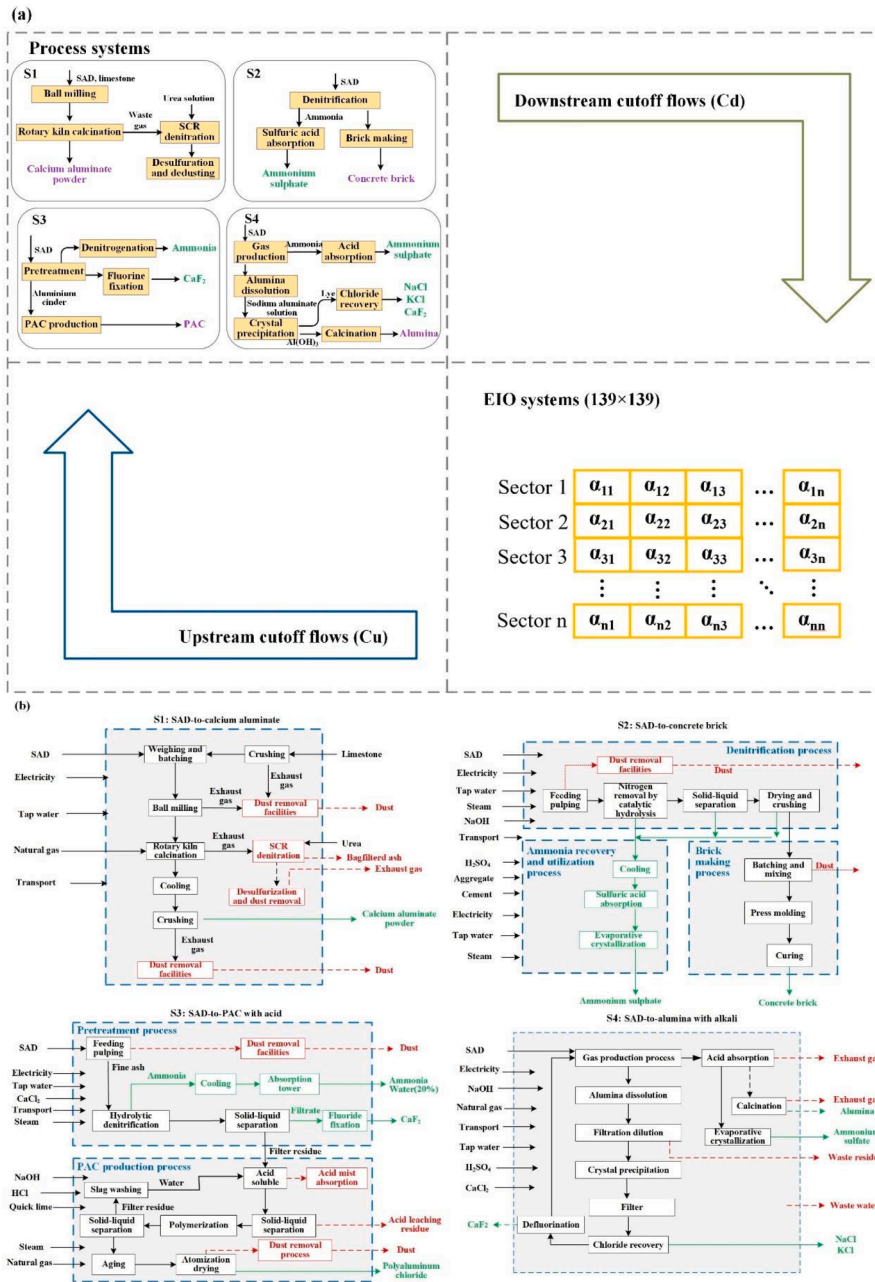


Fig. 1. (a) Structure of IHLCA model for SAD reutilization, including process systems, EIO systems, downstream cutoff flows, and upstream cutoff flows. (b) The system boundary and technological process of four SAD reutilization scenarios.

mate the environmental impacts of key life cycle processes, and the process system is complemented by the macroeconomic system. The process systems and the macroeconomic systems are integrated systematically by the upstream and downstream cutoff matrices (Zhao and You, 2019). According to Suh (2004), the environmental impact assessment based on IHLCA model can be expressed in Eq. (1):

$$E = [B_P \ B_{IO}] \begin{bmatrix} A_P & -C_d \\ -C_u & I - A_{IO} \end{bmatrix}^{-1} f \quad (1)$$

where  $E$  is the total environmental impact vector from process-based and EIO-based system.  $B_P$  denotes the direct environmental stressors per physical units in process system, and the coefficients of all input flows (e.g. kg CO<sub>2</sub>/kWh electricity) were obtained from Ecoinvent database v3.6 (Ecoinvent-Center, 2019).  $B_{IO}$  represents the environmental stressors by input-output commodities (e.g. kg CO<sub>2</sub> producing 10,000 CNY value of a

commodity), which is calculated by the CEEIO database (Liang et al., 2017). The structure of IHLCA model is shown in Fig. 1(a).  $A_P$  symbolizes the technology coefficient matrix for physical flows in process-based system (e.g., physical amount of electricity per ton of SAD reutilization).  $A_{IO}$  is established according to the China Input-Output Table 2012 denoting the commodity-by-commodity direct requirement coefficient matrix that excludes the portion of commodity flows already covered by process-based system.  $C_u$  represents the upstream cut-off flows in which a negative sign represents flow from input-output system to process system while  $C_d$  includes downstream cut-off flow from process system to input-output system (e.g., kg NaCl consuming per unit of monetary value of output).  $f$  is the final demand column indicating the amount of final product that is produced per functional unit.

A Five-step approach proposed by (Wiedmann et al., 2011) were used to construct  $C_u$ , which has been widely used in studies (Gao and You, 2017; Li et al., 2020). Notably, all bottom-up data were converted

into monetary unit in 2012 constant producers' price following the ratio of producers' price to purchasers' price (Table A3.1.) for  $C_u$  construction. Since the economic scale of the SAD reutilization system is negligible compared to the EIO system for China,  $C_d$  in this study was set as zero (Peters and Hertwich, 2006).

### 2.4. Impact assessment

CML 2001 was chosen to assess environmental impact of SAD reutilization, considering Global Warming potential (GWP), Human toxicity potential (HTP), Freshwater aquatic ecotoxicity (FAETP), Marine aquatic ecotoxicity (MAETP), Terrestrial ecotoxicity (TETP), Photochemical oxidation (POCP), Acidification potential (AP), Eutrophication (EP), Abiotic depletion (ADP) (Guinée, 2001). Besides, the Primary energy demand (PED) and Water use (WU) were used to investigate the energy and water consumption. The former includes consumption of all renewable and nonrenewable energy, and the latter indicates the use of freshwater resources (Ding et al., 2022).

The production cost assessment was conducted to compare the economic performances of SAD reutilization scenarios, which can be calculated by Eq. (2) (Liao et al., 2019; Zheng et al., 2022):

$$TC = C * X = C * \left[ I - \begin{pmatrix} A_p & -C_d \\ -C_u & I - A_{IO} \end{pmatrix} \right]^{-1} * f \tag{2}$$

Where  $TC$  is the total production cost,  $C = (c_1, c_2, \dots, c_k, c_{k+1} \dots c_{k+n})$ , where the first  $(k - 1)$  elements represent the unit of the processes, and the  $c_k$  is the cost of main production factors, including depreciation, labor and tax subsidies (Nakamura and Kondo, 2006), and remaining elements corresponding to  $n$  economic sectors is unity, because the input and output of these sectors were defined in monetary units. Therefore, the direct production cost can be calculated by Eq (3):

$$DC_k = (c_1, c_2, \dots, c_{k-1}) * \begin{pmatrix} a_{1,k} \\ a_{2,k} \\ \vdots \\ a_{k-1,k} \end{pmatrix} + \sum_{i=k+1}^{k+n} a_{i,k} + c_k \tag{3}$$

where  $DC_k$  is the direct production cost, and  $a_{i,k}, i \in (1, k+n)$  is the elements in  $A_{hybrid}$ .

### 2.5. Uncertainty and sensitivity analysis

Uncertainty in LCA can be classified into parameter uncertainty, scenario uncertainty, and model uncertainty (Gregory et al., 2016). In this study, we considered the uncertainty of four types of parameters (Table 1): (1) Input of energy and materials, including electricity, natural gas, water, chemicals, etc.; (2) transportation distance of raw materials, including SAD and other raw and auxiliary materials; (3) the unit

**Table 1**  
Parametric probability distributions of parameters.

Parameters	Description	Distribution	Bound/ coefficient of variation	Reference
$I$	Input of energy and material	Triangular distribution	[0.8i, i, 1.2i]	Enterprise interview
$D$	Transportation distance of raw materials	Uniform distribution	[50, 250] (km)	Enterprise interview
$P$	Product price	Triangular distribution	[0.5p, p, 1.5p]	(Li et al., 2020)
$B$	Environmental emissions and resource consumption per physical unit	Normal distribution	Coefficient variation=10%	(Ciroth et al., 2013)

price of products generated in SAD reutilization scenarios; and (4) Environmental emissions and resource consumption per physical unit.

The sensitivity analysis aims to describe the contribution of parameters to the uncertainty of the results. Global Sensitivity Analysis (GSA) explores the effects of the overall range of variation of input variables on the uncertainty of the results (Patouillard et al., 2019). In this study, we selected the standard regression coefficient method (Groen et al., 2016). All types of parameters in this study are independent. The variance explained by each of the parameter can be given by Eq (4):

$$S_j = \frac{var(E(g|p_j))}{var(g)} \tag{4}$$

where the ratio  $S_j$  is the sensitivity index, the  $var(E(g|p_j))$  is the conditional variance, which means "the expected reduction in variance that would be obtained if parameter  $p_j$  could be fixed" (Saltelli et al., 2010).

And when the parameter and output are linear,  $var(E(g|p_j)) = var(cp + c_0) = c^2 var(p)$ , where  $c, p$  are regression coefficient of  $g$  that are obtained by fitting. The  $var(g)$  is the variance of output result.

## 3. Results and discussion

### 3.1. Environmental impact

Fig. 2(a) presents the midpoint results of four SAD reutilization scenarios with the IHLCA model, with the environmental impact of the offsetting system subtracted. The environmental impacts of the SAD-to-alumina with alkali scenario (S4) with multi-component recovery were the smallest in most categories except for HTP, ADP and AP. In contrast, the SAD-to-PAC with acid scenario (S3), which is also a multi-component recycling method, has the worst environmental impact except for FAETP and MAETP. However, the environmental performances of single-component (S1) and two-component recovery (S2) scenarios in most categories were between S4 and S3. In addition, the total environmental impacts obtained by the normalization of all midpoint indicators illustrated in Table A4.1 is similar with the comparison of each indicator. The SAD-to-alumina with alkali scenario (S4) has the lowest environmental impact, followed by SAD-to-calcium aluminate (S1), SAD-to-concrete brick (S2), and SAD-to-PAC with acid (S3).

Particularly, IHLCA captures larger environmental impacts when compared to PLCA. The significant contributions from EIO-based systems were observed in categories including HTP, AP, and FAETP, accounting for 68.62–97.00%, 1.65–32.51%, and 7.74–98.09%, respectively. Furthermore, the contribution of EIO systems varies in each SAD scenario, for example, the midpoint results of S1 and S4 have relatively larger contributions from EIO-based systems. Nevertheless, for this SAD reutilization comparison study, the environmental impact comparison ranking results obtained by the IHLCA system are consistent with those just captured by the process-based system, except for the HTP indicator. But the significance of the EIO system's contribution cannot be ignored, which helps decision-makers identify the potential influence of these SAD reutilization scenarios on the entire economy.

Fig. 2(b) depicts the sectoral contributions of four hotspot indicators (EP, POCP, MAETP, and GWP) in SAD reutilization scenarios. POCP and EP were the two midpoint indicators with the highest normalized results, while GWP and MAETP had the highest impact values before normalization. For POCP and EP indicator, the sector "chemical products" was the largest contributor to SAD reutilization, except for S1 with single-component recovery, which only accounted for 0.5 and 1.4%, respectively. For S2 and S4, the chemical products sector brings significant offsetting effects in POCP and EP with the 44.38–55.75% and 48.1–38.03% respectively, resulting from avoided traditional by-product production. In addition to Al recovery like in S1, S2 recovers element N to produce ammonium sulfide, and S4 recycles elements N

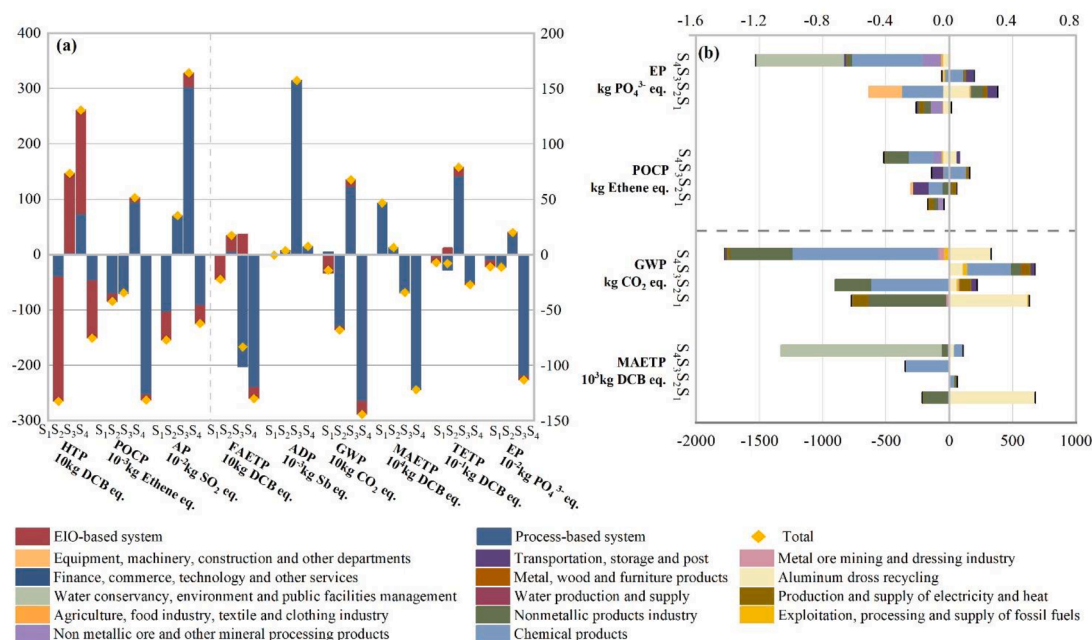


Fig. 2. (a): Midpoint results of integrated hybrid life cycle assessment for SAD reutilization. S1 (SAD-to-calcium aluminate); S2 (SAD-to-concrete brick); S3 (SAD-to-PAC with acid); S4 (SAD-to-alumina with alkali). (b): Sectoral contribution of EP, POCP, GWP and MAETP in SAD reutilization scenarios.

and F to produce four by-products (calcium fluoride, potassium chloride, sodium chloride, and ammonium sulfide). Although S3 has recovered the similar components as S4, avoiding conventional production of by-products such as CaF<sub>2</sub> and ammonia water is not enough to offset the huge environmental impact due to the large amount of hydrochloric acid required for PAC production. In addition, remarkable contributions from the construction sector, non-metallic products sector and water conservation, environment, and public facilities management sector were also observed in EP and POCP. In the SAD-to-concrete brick scenario (S2), the contribution of the construction sector accounts for 44.25% of the EP indicator due to the production of concrete bricks. Owing to the by-products of calcium aluminate and alumina in S1 and S4, the impact contribution of the sector "non-metallic products industry" to POCP was 31.42% and 41.36%, respectively. Additionally, the sector "water conservation, environment, and public facilities

management" contributes almost half of the impact offsets due to the avoidance of red mud disposal in traditional alumina production for EP of S4.

Fig. 2(b) shows that the GWP contribution of the SAD reutilization sector was significant for each scenario, particularly for S1 and S4 with the high temperature calcination process, which emitted 620 kg and 330.37 kg CO<sub>2</sub> eq., respectively. Furthermore, the chemicals sector brings significant offsets for S2 and S4 (S2: -620.20 kg CO<sub>2</sub> eq.; S4: -1153.29 kg CO<sub>2</sub> eq.) caused by traditional product substitution, while increases the GWP value for S3 (347.36 kg CO<sub>2</sub> eq.) due to hydrochloric acid consumption. As a result of offsets from the chemicals sector, the S4 has the lowest GWP value (-1443.87 kg CO<sub>2</sub> eq.). Reciprocally, the chemicals products sector saw a significant MAETP offset for S3 (-347,261.8 kg DCB eq.) while S2 (4315.3 kg DCB eq.) and S4 (66,718.04 kg DCB eq.) increased. The differential is mainly due to the

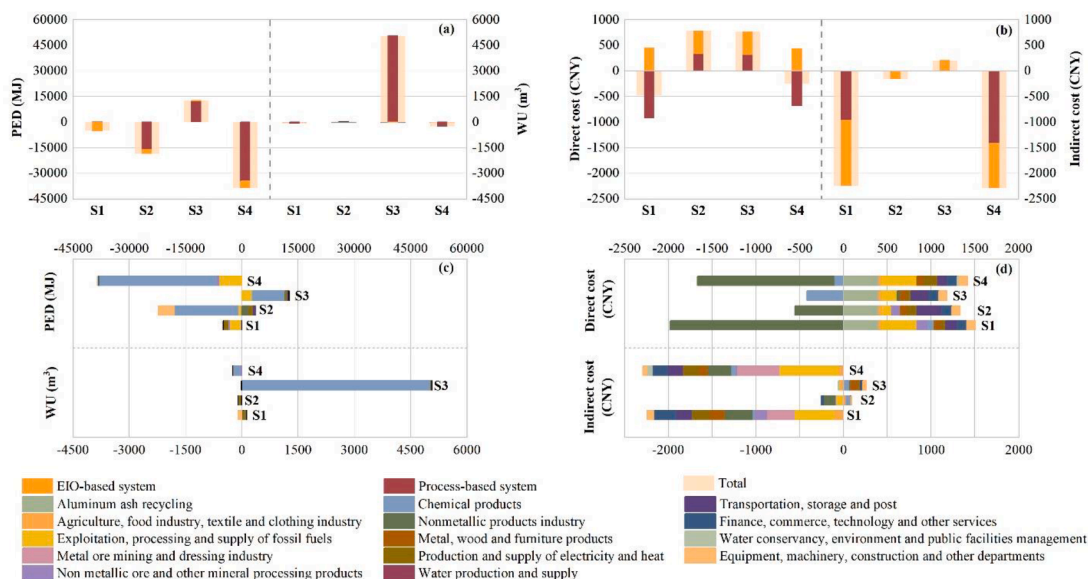


Fig. 3. Resource consumption, production costs, and sectoral contributions to SAD reutilization scenarios.

avoidance of the extremely high marine toxicity effects brought by the traditional PAC production process in S3. Meanwhile, the avoided MAETP impacts provided by products in S2 and S4 are not large enough to offset the impact caused by sulfuric acid and other chemical product consumption for SAD recovery.

### 3.2. The resource consumption and production cost of SAD reutilization

Fig. 3(a) shows that the lowest resource consumption of PED and WU was observed in the SAD-to-alumina with alkali scenario (S4) with multi-component recovery, while the SAD-to-PAC with acid scenario (S3), which is also a multi-component recycling method, has the worst performance. In scenarios S2, S3, S4, precess-based system captured most of the resource consumption, while the contribution of EIO-based system is just in the ranged of 2.40–13.31% and 0.02–0.68% for PED, and WU respectively. However, for the single component recovery scenario (S1), the EIO-based system makes a dominant contribution to PED with 95.14% owing to the limited inputs of materials and offsetting impact of calcium aluminate. As shown in Fig. 3(c), the sector "chemical products" accounts for a significant offsetting of S4, since the by-product ammonium sulfate avoids the resource required during the traditional manufacturing process. Particularly, the WU of S3 is as high as 505.61 m<sup>3</sup>, whereas that of other scenarios ranges from -24.34 to 3.08 m<sup>3</sup>, with absolute values less than one twentieth of S3. The huge differences are caused by HCl consumption, whose production requires a large amount of water.

As shown in Fig. 3(b), the single-component recovery scenario S1 is the optimal scenario to be recommended, with the lowest production cost of -271.36 yuan. Although only aluminum was recovered in this simple process, the highly valued by-product of calcium aluminate contributed a large part of the production cost offset. As for the multi-component recovery scenarios, S4 has a lower production cost of

-254.10 yuan due to the high-valued by-products, whereas S3 with low-valued PAC recycled has the highest production cost of 96.64 yuan. Therefore, when considering the economic dimension, decision-makers should not blindly pursue more component recovery but pay attention to the improvement of the quality and value of the recycled products. In addition, EIO-based systems have a significant impact on indirect production costs that cannot be ignored (Fig. 3b) (38.23–99.99%). The cost offsetting of S1 and S4 is primarily due to reduced consumption of fossil fuels and bauxite because of calcium aluminate and alumina recycling. Correspondingly, the contribution of offsetting in the sectors "exploitation, processing, and supply of fossil fuels" and "metal ore mining and dressing industry" was observed at 34.58% and 50.38%, respectively.

### 3.3. Uncertainty and sensitivity analysis

The probability distributions of all indicators for four scenarios are represented in Fig. 4, with the median and quartile values displayed in the box plot inside the violin. The thickness of the violin shape can be used to calculate the frequency of sample points. In particular, because x-axis units are corresponding physical units of indicators (e.g., kg SO<sub>2</sub> eq. AP), we cannot compare y-axis position among categories (Li et al., 2020). All indicators exhibit a bell-shaped curve, indicating that the outcome of IHLCA is stable and reliable. The huge span of sample points indicates the variability of indicators and accordingly provides opportunities for reducing environmental impact or cost. The results show that the span of each indicator in different schemes is basically similar. For example, in four scenarios, the ADP spans are 0.59 – 1.39, 0.68 – 1.36, 0.32 – 1.76, and 0.46 – 1.69 times the determined value, respectively. It's worth noting that the GWP, FAETP, and POCP of S1 and the ADP, EP, and HTP of S2 have a larger fluctuation range due to more parameter uncertainty sources. Consequently, these indicators have a greater potential to be mitigated and should be given more attention.

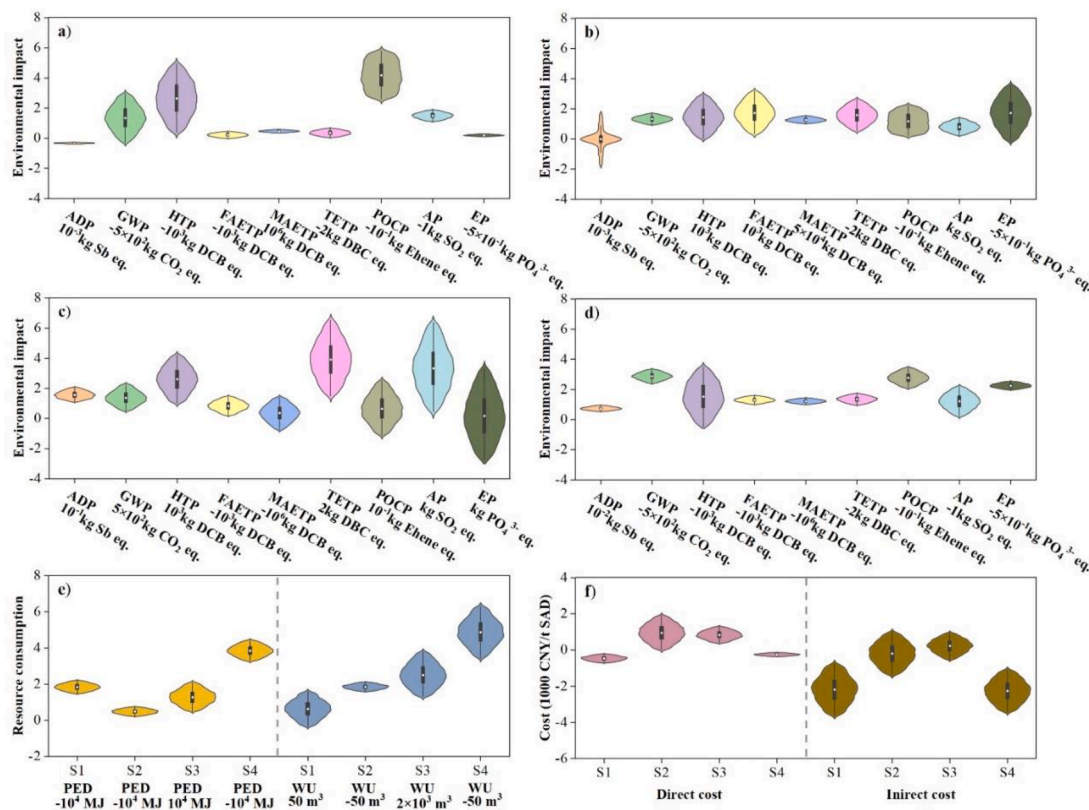


Fig. 4. A violin plot of environmental impact, resource consumption, and production cost for SAD reutilization scenarios with the Monte Carlo simulation (10,000 runs). a), b), c), and d) are the environmental impact results of S1, S2, S3, and S4, respectively; e) and f) are the simulation results of resource consumption and production cost, respectively.

The global sensitivity indexes are illustrated in Fig. 5, which represents how much the output variance is explained by key parameters (Patouillard et al., 2019). For indicators belonging to environmental impact and resource consumption, the variance in direct emissions and resource consumption for unit processes has a dominant sensitivity impact with a range of 46.90%–99.99% and 62.6%–94.3%, respectively. In addition, fluctuations in input parameters (energy and material consumption) should be noted. For S2, the parameter "input of energy and material" has sensitivity impacts of 38.39% and 21.45% on MAETP and AP, which may be due to high consumption of sulfuric acid and cement. Meanwhile, the sensitivity indexes for "energy and material input" for all indicators in S3 range from 10.54% to 41.59%.

The price fluctuations of the by-product caused by market acceptance uncertainty have been proven to have a significant impact on the LCA results (Russo et al., 2019; Wang et al., 2022). Notably, the variation in "price of by-product" has a larger impact on production costs, with a sensitivity index of 53.42–90.98%. Of the four possible by-products of the four technologies, NaCl and PAC prices are the most affected by the market and they remain depressed due to overcapacity. In S3, "input of energy and material" contributes 39.08% and 43.04% of the sensitivity indexes for direct and indirect cost, respectively, due to the high consumption of hydrochloric acid, calcium chloride, and other reagents. Hence, adding more value to the by-products generated in SAD reutilization process is the first priority to maximize economic benefits. Furthermore, changes in parameters like emission and resource consumption per physical unit have no impact on production costs. Since the production cost mentioned in this study is an internal cost, it does not include the external cost caused by environmental emissions.

Additionally, "transportation distance" has little effect on all indicators of environmental impacts, resource consumption, and production cost. The direct emission from transportation is relatively low in a process-based system (e.g., for S2 scenario, 1 t of cement production releases 736 kg of CO<sub>2</sub> equivalent GWP, which is approximately 8205 times that of 1 t-km of raw material transportation, 0.897 kg CO<sub>2</sub> eq.).

Moreover, the transportation cost in the SAD reutilization scenario is about 0.6 yuan/t-km, while the by-product, such as calcium aluminate, is worth about 1800 yuan/t. As a result of such a large cost disparity, the influence of transportation distance change is limited.

### 3.4. Implications

IHLCA captures larger impacts than PLCA. In comparative SAD reutilization studies, significant contributions from EIO-based systems were observed, indicating that IHLCA can avoid system truncation by constructing upstream and downstream matrices to expand the system boundary to the entire economy. For SAD reutilization, the contribution of the EIO-based system cannot be ignored, especially for the HTP, FAETP, and AP indicators, with contribution rates of 68.62–97.00%, 1.65–32.51%, and 7.74–98.09%, respectively. Additionally, the EIO-based systems also have a significant impact on production costs, with a contribution rate of 38.23–99.99%.

Whether multi-component recovery from SAD is the best choice or not depends on the added value of by-products and the market demand. In this work, the multi-component recovery scenario, SAD-to-PAC with acid, was the worst option in terms of environmental impact, resource consumption, and production cost due to the massive use of hydrochloric acid. In contrast, SAD-to-calcium aluminate with single-component recovery stands out due to its best economic performance and suboptimal environmental performance, followed by the two-component recovery scenario (SAD-to-concrete brick). Notably, S1, S2, and S3 have not considered the chlorine salt recovery due to the low market acceptability of industrial salt. However, if a market shortage of these by-products occurs and the resulting by-product price rises enough to offset the cost of other raw materials in the production process, the finer component separation and utilization of SAD will form a new investment hotspot. Therefore, further analysis of multi-component recovery scenarios is required in the case of positive market acceptability.

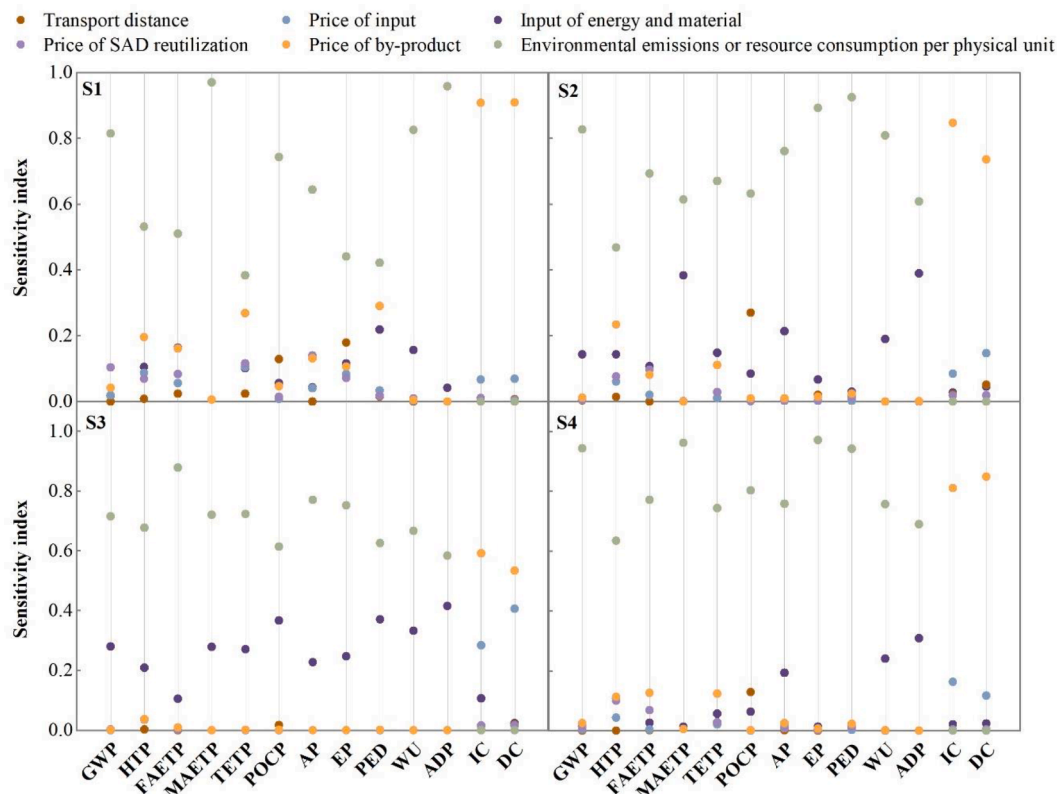


Fig. 5. The sensitivity analysis of four SAD reutilization scenarios.

#### 4. Conclusions

This is the first comparative study of four emerging SAD reutilization technologies by the IHLCA model from the multiple perspectives of environmental impact, resource consumption, and economic performance. In this study, the trade-offs between multi-component recovery and multi-dimension impact assessment for SAD reutilization were revealed. SAD-to-alumina with alkali was found to have the smallest environmental impact and resource consumption, while SAD-to-calcium aluminate was considered to achieve the highest economic profit. The SAD-to-PAC with acid process was the worst option due to the massive use of hydrochloric acid, although three by-products (PAC, CaF<sub>2</sub>, and ammonia) were generated. Furthermore, combining the results of the sensitivity analysis, the production costs is most sensitive to the fluctuation in market price of by-products. Therefore, it is suggested to choose the recycling path which generates by-products with high added value and market acceptance. Moreover, the industrial salts and PAC generated from SAD reutilization process need more attention due to their low market acceptance and narrow application scenarios.

Although the current study provides a new perspective and specific technical selection advice for the industrialization of SAD reutilization, limitations still exist. The data for the life cycle inventory were gathered from a field survey of specific enterprises, which may have differences in actual industrial production in different regions. Given regional differences in SAD disposal, energy consumption structure, and Al-products demand, more research on region-specific suggestions in the selection of suitable SAD reutilization pathways and national policy-making to promote interprovincial collaboration to reduce secondary aluminum industry-related environmental impacts is required.

#### CRedit authorship contribution statement

**Luying Xiao:** Conceptualization, Methodology, Writing – original draft. **Yao Wang:** Conceptualization, Methodology, Writing – original draft, Writing – review & editing. **Rufeng Zheng:** Methodology, Visualization. **Jingru Liu:** Methodology, Writing – review & editing. **Jun Zhao:** Resources, Visualization. **Tek Maraseni:** Writing – review & editing. **Guangren Qian:** Conceptualization, Methodology, Supervision, Writing – review & editing, Funding acquisition.

#### Declaration of Competing Interest

The authors declare that they have no known competing financial interests or personal relationships that could have appeared to influence the work reported in this paper.

#### Data availability

Data will be made available on request.

#### Acknowledgments

This study was funded by the National Key Research and Development Program of China (No. 2019YFC1906900).

#### Supplementary materials

Supplementary material associated with this article can be found, in the online version, at [doi:10.1016/j.resconrec.2023.106987](https://doi.org/10.1016/j.resconrec.2023.106987).

#### References

Ciroth, A., Muller, S., Weidema, B., Lesage, P., 2013. Empirically based uncertainty factors for the pedigree matrix in ecoinvent. *Int. J. Life Cycle Assess.* 21 (9), 1338–1348. <https://doi.org/10.1007/s11367-013-0670-5>.

- Dash, B., Das, B.R., Tripathy, B.C., Bhattacharya, I.N., Das, S.C., 2008. Acid dissolution of alumina from waste aluminium dross. *Hydrometallurgy* 92 (1–2), 48–53. <https://doi.org/10.1016/j.hydromet.2008.01.006>.
- Ding, J., Hu, X., Feng, Z., Dong, L., 2022. Environmental life cycle assessment of monosodium glutamate production in China: based on the progress of cleaner production in recent ten years. *Sci. Total Environ.* 818, 151706 <https://doi.org/10.1016/j.scitotenv.2021.151706>.
- Ding, N., Liu, N., Lu, B., Yang, J., 2021. Life cycle greenhouse gas emissions of aluminum based on regional industrial transfer in China. *J. Ind. Ecol.* 25 (6), 1657–1672. <https://doi.org/10.1111/jiec.13146>.
- Ecoinvent-Center, 2019. Ecoinvent Database v3.6. <http://www.ecoinvent.org>.
- Elshkaki, A., Graedel, T.E., Ciacci, L., Reck, B.K., 2018. Resource demand scenarios for the major metals. *Environ. Sci. Technol.* 52 (5), 2491–2497. <https://doi.org/10.1021/acs.est.7b05154>.
- Gao, J., You, F., 2017. Integrated hybrid life cycle assessment and optimization of shale gas. *ACS Sustain. Chem. Eng.* 6 (2), 1803–1824. <https://doi.org/10.1021/acssuschemeng.7b03198>.
- Gregory, J.R., Noshadravan, A., Olivetti, E.A., Kirchain, R.E., 2016. A methodology for robust comparative life cycle assessments incorporating uncertainty. *Environ. Sci. Technol.* 50 (12), 6397–6405. <https://doi.org/10.1021/acs.est.5b04969>.
- Groen, E.A., Bokkers, E.A.M., Heijungs, R., de Boer, L.J.M., 2016. Methods for global sensitivity analysis in life cycle assessment. *Int. J. Life Cycle Assess.* 22 (7), 1125–1137. <https://doi.org/10.1007/s11367-016-1217-3>.
- Guinée, J., 2001. Handbook on life cycle assessment — operational guide to the ISO standards. *Int. J. Life Cycle Assess.* 6 (5) <https://doi.org/10.1007/bf02978784>, 255–255.
- Hazar, A.B.Y., Saridede, M.N., Cigdem, M., 2005. A study on the structural analysis of aluminium drosses and processing of industrial aluminium salty slags. *Scand. J. Metallurgy* 34 (3), 213–219. <https://doi.org/10.1111/j.1600-0692.2005.00732>.
- Hiraki, T., Takeuchi, M., Hisa, M., Akiyama, T., 2005. Hydrogen production from waste aluminum at different temperatures, with LCA. *Mater. Trans.* 46 (5), 1052–1057. <https://doi.org/10.2320/matertrans.46.1052>.
- Hong, J.-p., Wang, J., Chen, H.-y., Sun, B.-d., Li, J.-j., Chen, C., 2010. Process of aluminum dross recycling and life cycle assessment for Al-Si alloys and brown fused alumina. *Trans. Nonferrous Metals Soc. China* 20 (11), 2155–2161. [https://doi.org/10.1016/s1003-6326\(09\)60435-0](https://doi.org/10.1016/s1003-6326(09)60435-0).
- Hu, S., Wang, D., Hou, D., Zhao, W., Li, X., Qu, T., Zhu, Q., 2021. Research on the preparation parameters and basic properties of premelted calcium aluminate slag prepared from secondary aluminum dross. *Materials (Basel)* 14 (19). <https://doi.org/10.3390/ma14195855>.
- Huber, F., Fellner, J., 2018. Integration of life cycle assessment with monetary valuation for resource classification: the case of municipal solid waste incineration fly ash. *Resour., Conserv. Recycl.* 139, 17–26. <https://doi.org/10.1016/j.resconrec.2018.08.003>.
- Kuo Cheng, H., Ueng, T.H., Chen, C.C., 2013. A study of stabilization and recycling for aluminum dross. *Appl. Mech. Mater.* 275–277, 2237–2240. <https://doi.org/10.4028/www.scientific.net/AMM.275-277.2237>.
- Li, F., Jiang, J.-Q., Wu, S., Zhang, B., 2010. Preparation and performance of a high purity poly-aluminum chloride. *Chem. Eng. J.* 156 (1), 64–69. <https://doi.org/10.1016/j.cej.2009.09.034>.
- Li, P., Zhang, M., Teng, L., Seetharaman, S., 2012. Recycling of aluminum salt cake: utilization of evolved ammonia. *Metall. Mater. Trans. B* 44 (1), 16–19. <https://doi.org/10.1007/s11663-012-9779-3>.
- Li, S., Qin, Y., Subbiah, J., Dvorak, B., 2020a. Life cycle assessment of the U.S. beef processing through integrated hybrid approach. *J. Clean. Prod.* 265 <https://doi.org/10.1016/j.jclepro.2020.121813>.
- Li, Y., Yue, Q., He, J., Zhao, F., Wang, H., 2020b. When will the arrival of China's secondary aluminum era? *Resour. Policy* 65. <https://doi.org/10.1016/j.resourpol.2019.101573>.
- Liang, S., Feng, T., Qu, S., Chiu, A.S.F., Jia, X., Xu, M., 2017. Developing the Chinese environmentally extended input-output (CEEIO) database. *J. Ind. Ecol.* 21 (4), 953–965. <https://doi.org/10.1111/jiec.12477>.
- Liao, M.-I., Shih, X.-H., Ma, H.-w., 2019. Secondary copper resource recycling and reuse: a waste input–output model. *J. Clean. Prod.* 239 <https://doi.org/10.1016/j.jclepro.2019.118142>.
- Mahinroosta, M., Allahverdi, A., 2018. A promising green process for synthesis of high purity activated-alumina nanopowder from secondary aluminum dross. *J. Clean. Prod.* 179, 93–102. <https://doi.org/10.1016/j.jclepro.2018.01.079>.
- Maung, K.N., Yoshida, T., Liu, G., Lwin, C.M., Muller, D.B., Hashimoto, S., 2017. Assessment of secondary aluminum reserves of nations. *Resour., Conserv. Recycl.* 126, 34–41. <https://doi.org/10.1016/j.resconrec.2017.06.016>.
- Meshram, A., Singh, K.K., 2018. Recovery of valuable products from hazardous aluminum dross: a review. *Resour., Conserv. Recycl.* 130, 95–108. <https://doi.org/10.1016/j.resconrec.2017.11.026>.
- Meyer, F.M., 2004. Availability of bauxite reserves. *Nat. Resour. Res.* 13 (3), 161–172. <https://doi.org/10.1023/B:NARR.0000046918.50121.2e>.
- Nakamura, S., Kondo, Y., 2006. A waste input–output life-cycle cost analysis of the recycling of end-of-life electrical home appliances. *Ecol. Econ.* 57 (3), 494–506. <https://doi.org/10.1016/j.ecolecon.2005.05.002>.
- Ni, H., Wu, W., Lv, S., Wang, X., Tang, W., 2021. Formulation of non-fired bricks made from secondary aluminum ash. *Coatings* 12 (1). <https://doi.org/10.3390/coatings12010002>.
- Padamata, S.K., Yasinskiy, A., Polyakov, P., 2021. A review of secondary aluminum production and its byproducts. *Jom* 73 (9), 2603–2614. <https://doi.org/10.1007/s11837-021-04802-y>.



- Palma-Rojas, S., Caldeira-Pires, A., Nogueira, J.M., 2015. Environmental and economic hybrid life cycle assessment of bagasse-derived ethanol produced in Brazil. *Int. J. Life Cycle Assess.* 22 (3), 317–327. <https://doi.org/10.1007/s11367-015-0892-9>.
- Patouillard, L., Collet, P., Lesage, P., Tirado Seco, P., Bulle, C., Margni, M., 2019. Prioritizing regionalization efforts in life cycle assessment through global sensitivity analysis: a sector meta-analysis based on ecoinvent v3. *Int. J. Life Cycle Assess.* 24 (12), 2238–2254. <https://doi.org/10.1007/s11367-019-01635-5>.
- Peters, G.P., Hertwich, E.G., 2006. A comment on “Functions, commodities and environmental impacts in an ecological-economic model”. *Ecol. Econ.* 59 (1), 1–6. <https://doi.org/10.1016/j.ecolecon.2005.08.008>.
- Russo, I., Confente, I., Scarpi, D., Hazen, B.T., 2019. From trash to treasure: the impact of consumer perception of bio-waste products in closed-loop supply chains. *J. Clean. Prod.* 218, 966–974. <https://doi.org/10.1016/j.jclepro.2019.02.044>.
- Saltelli, A., Annoni, P., Azzini, I., Campolongo, F., Ratto, M., Tarantola, S., 2010. Variance based sensitivity analysis of model output. Design and estimator for the total sensitivity index. *Comput. Phys. Commun.* 181 (2), 259–270. <https://doi.org/10.1016/j.cpc.2009.09.018>.
- Suh, S., 2004. Functions, commodities and environmental impacts in an ecological-economic model. *Ecol. Econ.* 48 (4), 451–467. <https://doi.org/10.1016/j.ecolecon.2003.10.013>.
- Suh, S., Huppes, G., 2005. Methods for life cycle inventory of a product. *J. Clean. Prod.* 13 (7), 687–697. <https://doi.org/10.1016/j.jclepro.2003.04.001>.
- Tenorio, J.A.S., Espinosa, D.C.R., 2002. Effect of salt/oxide interaction on the process of aluminum recycling. *J. Light Metals* 2 (2), 89–93. [https://doi.org/10.1016/s1471-5317\(02\)00027-5](https://doi.org/10.1016/s1471-5317(02)00027-5).
- Ünlü, N., Drouet, M.G., 2002. Comparison of salt-free aluminum dross treatment processes. *Resour., Conserv. Recycl.* 36 (1), 61–72. [https://doi.org/10.1016/s0921-3449\(02\)00010-1](https://doi.org/10.1016/s0921-3449(02)00010-1).
- Viau, S., Majeau-Bettez, G., Spreutels, L., Legros, R., Margni, M., Samson, R., 2020. Substitution modelling in life cycle assessment of municipal solid waste management. *Waste Manag.* 102, 795–803. <https://doi.org/10.1016/j.wasman.2019.11.042>.
- Wang, Y., Dong, J., Liu, J., Zheng, R., Yue, Y., Zhang, Y., Qian, G., 2022. Toward a sustainable municipal solid waste incineration fly-ash utilization network: integrating hybrid life cycle assessment with multiobjective optimization. *ACS Sustain. Chem. Eng.* 10 (23), 7635–7647. <https://doi.org/10.1021/acssuschemeng.2c01468>.
- Wiedmann, T.O., Suh, S., Feng, K., Lenzen, M., Acquaye, A., Scott, K., Barrett, J.R., 2011. Application of hybrid life cycle approaches to emerging energy technologies—the case of wind power in the UK. *Environ. Sci. Technol.* 45 (13), 5900–5907. <https://doi.org/10.1021/es2007287>.
- Yang, Z., Gao, B., Yue, Q., 2010. Coagulation performance and residual aluminum speciation of Al<sub>2</sub>(SO<sub>4</sub>)<sub>3</sub> and polyaluminum chloride (PAC) in Yellow River water treatment. *Chem. Eng. J.* 165 (1), 122–132. <https://doi.org/10.1016/j.cej.2010.08.076>.
- Yoo, S.-J., Yoon, H.-S., Jang, H.D., Lee, J.-W., Hong, S.-T., Lee, M.-J., Lee, S.-I., Jun, K.-W., 2006. Synthesis of aluminum isopropoxide from aluminum dross. *Korean J. Chem. Eng.* 23 (4), 683–687. <https://doi.org/10.1007/bf02706815>.
- Zarchi, I., Friedler, E., Rebhun, M., 2013. Polyaluminium chloride as an alternative to alum for the direct filtration of drinking water. *Environ. Technol.* 34 (9–12), 1199–1209. <https://doi.org/10.1080/09593330.2012.743594>.
- Zhang, X., 2021. 2022 China's secondary aluminum raw material supply and prospects for import and export trends (in Chinese). *Resour. Recycl.* (11), 24–26.
- Zhao, S., You, F., 2019. Comparative life-cycle assessment of li-ion batteries through process-based and integrated hybrid approaches. *ACS Sustain. Chem. Eng.* 7 (5), 5082–5094. <https://doi.org/10.1021/acssuschemeng.8b05902>.
- Zhao, X., Liu, Y., Lyu, G., Zhang, Y., Zhang, T.-a., 2022. Removal of fluorine, chlorine, and nitrogen from aluminum dross by wet process. In: Eskin, D. (Ed.), *Light Metals 2022*, Ed. Springer International Publishing, Cham, pp. 48–55.
- Zheng, R., Wang, Y., Liu, Z., Zhou, J., Yue, Y., Qian, G., 2022. Environmental and economic performances of municipal solid waste incineration fly ash low-temperature utilization: an integrated hybrid life cycle assessment. *J. Clean. Prod.* 340 <https://doi.org/10.1016/j.jclepro.2022.130680>.
- Zhu, X., Jin, Q., 2021. Comparison of three emerging dross recovery processes in china's aluminum industry from the perspective of life cycle assessment. *ACS Sustain. Chem. Eng.* 9 (19), 6776–6787. <https://doi.org/10.1021/acssuschemeng.1c00960>.
- Zhu, X., Jin, Q., Ye, Z., 2020. Life cycle environmental and economic assessment of alumina recovery from secondary aluminum dross in China. *J. Clean. Prod.* 277 <https://doi.org/10.1016/j.jclepro.2020.123291>.